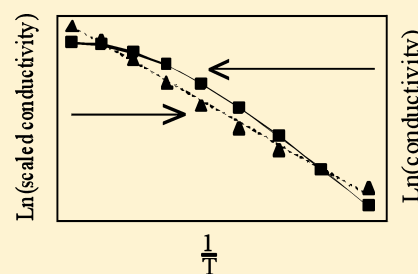


Ion Transport with Charge-Protected and Non-Charge-Protected Cations in Alcohol-Based Electrolytes Using the Compensated Arrhenius Formalism. Part I: Ionic Conductivity and the Static Dielectric Constant

Matt Petrowsky, Allison Fleshman, and Roger Frech*

Department of Chemistry and Biochemistry, University of Oklahoma, 101 Stephenson Parkway, Norman, Oklahoma 73019, United States

ABSTRACT: The temperature dependence of ionic conductivity and the static dielectric constant is examined for 0.30 *m* TbaTf- or LiTf-1-alcohol solutions. Above ambient temperature, the conductivity increases with temperature to a greater extent in electrolytes whose salt has a charge-protected cation. Below ambient temperature, the dielectric constant changes only slightly with temperature in electrolytes whose salt has a cation that is not charge-protected. The compensated Arrhenius formalism is used to describe the temperature-dependent conductivity in terms of the contributions from both the exponential prefactor σ_0 and Boltzmann factor $\exp(-E_a/RT)$. This analysis explains why the conductivity decreases with increasing temperature above 65 °C for the LiTf-dodecanol electrolyte. At higher temperatures, the decrease in the exponential prefactor is greater than the increase in the Boltzmann factor.



INTRODUCTION

A complete, detailed microscopic picture of mass and charge transport has yet to emerge for organic liquids and liquid electrolytes. Our previous work has explored transport phenomena by assuming that the solvent/solution static dielectric constant plays an integral role in governing the transport process.^{1–5} A compensated Arrhenius formalism (CAF) has been developed where the temperature-dependent transport property of interest (i.e., ionic conductivity, diffusion coefficient) assumes an Arrhenius-like expression with a static dielectric constant dependence in the exponential prefactor. This new formalism has been very successful in describing the experimental data for a wide variety of polar solvent families including the alcohols, ketones, and acetates.

Most of our conductivity studies to date have focused on tetrabutylammonium trifluoromethanesulfonate (TbaTf)-based liquid electrolytes because the monovalent nitrogen atom of the Tba cation is surrounded by bulky butyl groups that limit how closely a heteroatom (anion or solvent) can approach the positively charged nitrogen atom. Consequently, no discrete ionic species such as contact ion pairs or aggregates are observed in Tba-containing electrolytes on the time scale of IR spectroscopy.^{6–9} Due to the unique properties of the Tba cation, it is useful to distinguish two classes of ions although the distinction is not absolute; these are charge-protected and non-charge-protected. The Tba cation is charge-protected, also referred to as charge-shielded, in that only “free” ions exist in solution although long-range monopole–monopole interactions exist between Tba and the anion. Furthermore, the Tba–solvent heteroatom interaction is not strong enough to substantially affect the electronic distribution of the solvent

heteroatom, as evidenced by the failure to observe cation-dependent frequency shifts in the vibrational spectrum of the solvent molecules. In contrast to Tba, an excellent example of a non-charge-protected cation is the lithium ion. It is well-known that lithium trifluoromethanesulfonate (LiTf)-based electrolytes form discrete contact ion pairs and aggregates in addition to the lithium cation strongly coordinating the solvent heteroatom.^{6,7,10–12} Here, we apply the CAF to temperature-dependent conductivity data for 0.30 *m* salt-1-alcohol electrolytes, where the salt is either TbaTf or LiTf. The alcohols examined are butanol, pentanol, hexanol, heptanol, octanol, and dodecanol. Additionally, IR spectroscopy is used to probe the extent of ionic association in these systems. It will be shown that a charge-protected cation such as Tba can produce substantially different transport behavior compared to strongly interacting cations such as Li.

EXPERIMENTAL SECTION

All chemicals ($\geq 99\%$ pure) were obtained from either Aldrich or Alfa Aesar and used as received. The chemicals were stored, and all samples were prepared in a glovebox (≤ 1 ppm H_2O) under a nitrogen atmosphere. The liquid electrolytes were made at ambient glovebox temperature (approximately 27 °C) by dissolving salt into solvent until the appropriate molal concentration (moles salt/kg solvent) was obtained, followed by stirring for 24 h.

Received: September 23, 2011

Revised: April 13, 2012

Published: May 4, 2012

The capacitance (C) and conductance (G) were measured using a HP 4192A impedance analyzer that swept a frequency range from 1 kHz to 13 MHz. The sample holder was an Agilent 16452A liquid test fixture. The conductivity σ was calculated from the measured conductance G through the equation $\sigma = L \times G \times A^{-1}$, where L is the electrode gap and A is the electrode area. The static dielectric constant ϵ_s was calculated from the measured capacitance C through the equation $\epsilon_s = \alpha \times C \times C_0^{-1}$, where α is a variable to account for stray capacitance and C_0 is the vacuum capacitance.¹³ A Huber ministat 125 bath was used to regulate the temperature from 5 to 85 °C, in increments of 10 °C. Additional details of the conductivity/dielectric constant instrumentation and method of data analysis have been previously given.⁵

IR spectra were recorded on a Bruker IFS 66V FTIR spectrometer using a N_2 purge. The sample was contained between NaCl windows in a fully sealed Harrick temperature-controlled demountable liquid cell (model TFC-M25-3). The temperature was regulated using both a Neslab coolflow CFT-33 refrigerated recirculator and an Omega CN9000A digital temperature controller. The spectral resolution was 1 cm^{-1} , and each spectrum resulted from 64 scans. Curve fitting was performed with Galactic Grams version 5.2 using Gaussian functions and a linear baseline.

RESULTS AND DISCUSSION

1. Static Dielectric Constant Data. CAF-based studies have underscored the importance of the solution static dielectric constant in charge and mass transport.^{1–5} The addition of salt to a pure polar liquid can significantly change the value of the static dielectric constant.^{5,14–16} Both the amount and type of salt affects the magnitude as well as the temperature dependence of the dielectric constant. Figure 1

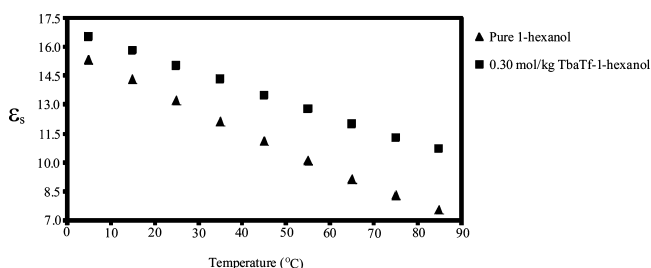


Figure 1. Static dielectric constant versus temperature for pure 1-hexanol and for 0.30 *m* TbaTf-1-hexanol solution.

shows that the addition of TbaTf to 1-hexanol increases the magnitude of the dielectric constant at each temperature shown. The dielectric constant decreases approximately linearly with temperature for both pure 1-hexanol ($R^2 = 0.9972$ linear fit) and 0.30 *m* TbaTf-1-hexanol ($R^2 = 0.9993$ linear fit). However, the difference in slope between the two sets of data in Figure 1 clearly illustrates that the addition of TbaTf prevents the dielectric constant from decreasing with temperature to the same extent as for pure hexanol.

In contrast to the data in Figure 1, the qualitative temperature dependence of the dielectric constant for certain 1-alcohol electrolytes can differ from that observed for the pure solvent. Figure 2 shows the temperature dependence of the dielectric constant over the range of 5–85 °C for four different 0.30 *m* 1-hexanol electrolytes. Tetrabutylphosphonium tetrafluoroborate (TbpBF₄) and TbaTf have charge-protected

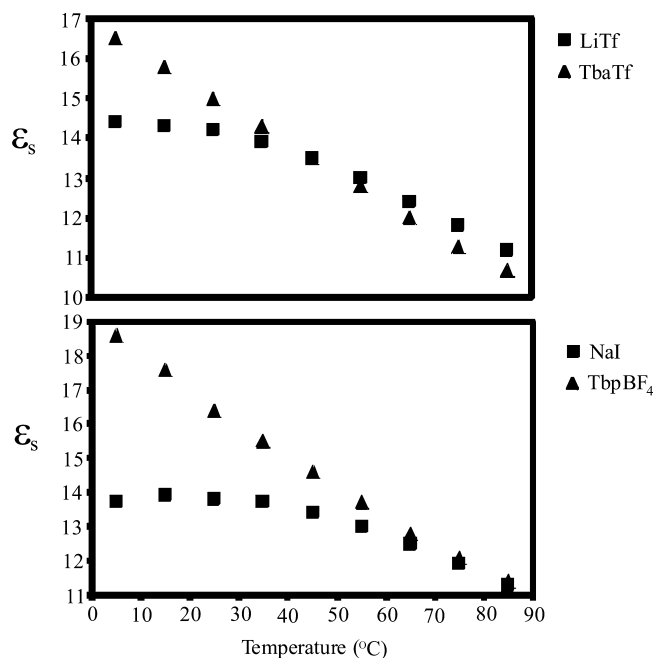


Figure 2. Static dielectric constant versus temperature for 0.30 *m* MX-1-hexanol solutions (MX = TbaTf, LiTf, NaI, or TbpBF₄).

cations, while sodium iodide and LiTf are not charge-protected. The greatest disparity between the charge-protected and non-charge-protected salts occurs at lower temperatures where the values of the dielectric constant for LiTf and NaI are markedly lower than those of TbaTf and TbpBF₄. The non-charge-protected salts have dielectric constants that change only slightly with temperature from 5 to 25 °C. The dielectric constant does decrease to a much greater extent for higher temperatures, which leads to decidedly nonlinear behavior for the temperature-dependent dielectric constant of the LiTf and NaI solutions. Similarly to the TbaTf data, the dielectric constant for the TbpBF₄ electrolyte decreases linearly with temperature ($R^2 = 0.9947$ linear fit), although for a given temperature, the value of the dielectric constant for the TbpBF₄ solution is slightly larger than that for TbaTf. The data in Figure 2 suggest that the classification of salts as either charge-protected or non-charge-protected is useful for characterizing the temperature-dependent dielectric constant for 1-alcohol electrolytes. It is not clear why a non-charge-protected cation greatly reduces the temperature dependence of the dielectric constant at low temperatures for 1-alcohol electrolytes, but it might be at least partly due to the interaction of the cation with the hydrogen-bonding network of the alcohol. It is well-known that 1-alcohols at low temperatures have extended hydrogen-bonded chain structures where the majority of the alcohol hydroxyl groups experience hydrogen bonding-interactions from both the oxygen and hydrogen atoms.^{17,18} Understanding the process by which a strongly coordinating cation interacts with a hydrogen-bonding network would undoubtedly provide insight into the dielectric constant behavior of Figure 2.

2. Conductivity Data. Similarly to the dielectric constant data already shown, the qualitative temperature-dependent behavior of the conductivity is affected by the nature of the salt. The top half of Figure 3 plots the conductivity against the temperature for 0.30 *m* 1-hexanol solutions where the salt is either TbaTf or LiTf. The conductivities of the two solutions are very similar at low temperatures, but they begin to deviate

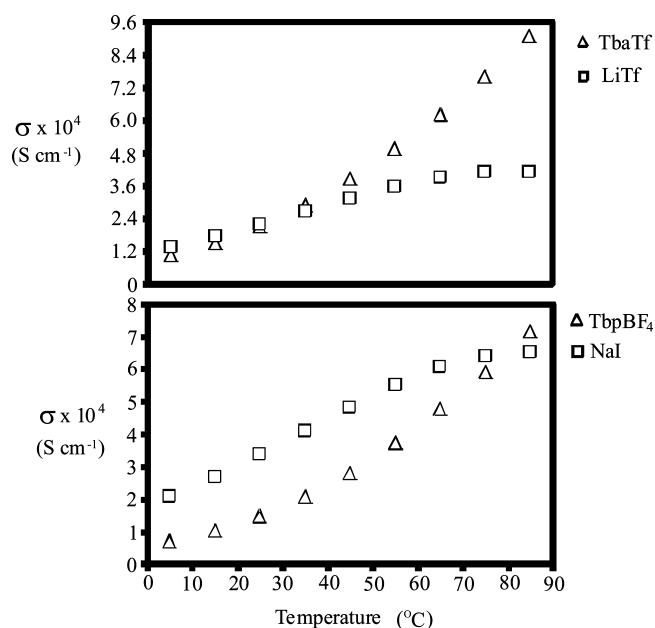


Figure 3. Conductivity versus temperature for 0.30 *m* MX-1-hexanol solutions (MX = TbaTf, LiTf, NaI, or TbpBF₄).

from each other at approximately 45 °C. The conductivity of the TbaTf solution continues to increase with temperature at elevated temperatures, while that for the LiTf solution levels off. The bottom half of Figure 3 shows that the conductivity for the NaI electrolyte begins to plateau above 70 °C, while that for the TbpBF₄ solution continues to increase. The fact that the conductivity plateaus at lower temperatures for the LiTf and NaI solutions implies that a distinction can be made between the transport of charge-protected and non-charge-protected salts in 1-alcohol electrolytes. In the following section, the CAF will be utilized to help interpret the temperature-dependent conductivity data shown in Figure 3.

3. CAF Analysis of Conductivity Data. The CAF assumes the ionic conductivity has the form

$$\sigma = \sigma_0(\epsilon_s(T)) \exp(-E_a/RT) \quad (1)$$

where σ is the ionic conductivity, $\sigma_0(\epsilon_s(T))$ is the exponential prefactor, ϵ_s is the static dielectric constant, T is temperature, R is the gas constant, and E_a is the activation energy. In eq 1, the exponential prefactor is written to emphasize its functional dependence on a temperature-dependent static dielectric constant. A scaling procedure can be performed to “compensate” for the temperature dependence of the exponential prefactor.¹ The end result of the scaling process is the compensated Arrhenius equation (CAE)

$$\ln\left(\frac{\sigma(T, \epsilon_s)}{\sigma_r(T_r, \epsilon_s)}\right) = \frac{-E_a}{RT} + \frac{E_a}{RT_r} \quad (2)$$

where $\sigma(T, \epsilon_s)$ is the temperature-dependent conductivity, $\sigma_r(T_r, \epsilon_s)$ is the reference conductivity, and T_r is the reference temperature. From eq 2, a graph of $\ln[\sigma(T, \epsilon_s)/\sigma_r(T_r, \epsilon_s)]$ versus $1/T$ is linear if the data follow CAE behavior. The activation energy is calculated from either the slope or the y -intercept.

Figure 4 shows that the simple Arrhenius plot for 0.30 *m* LiTf-1-hexanol is distinctly nonlinear over the temperature range of 5–85 °C. Also shown in Figure 4 is a compensated Arrhenius plot for 0.30 *m* LiTf-1-hexanol scaled to reference

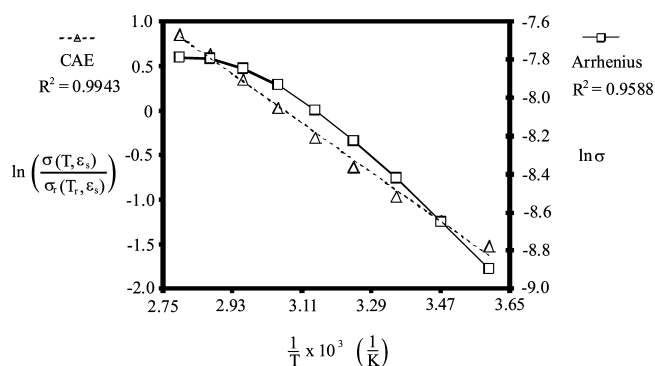


Figure 4. Simple Arrhenius plot and compensated Arrhenius plot for 0.30 *m* LiTf-1-hexanol.

data at 55 °C. The reference curve consists of the 55 °C conductivities and dielectric constants of five members, 0.30 *m* LiTf solutions of 1-butanol, 1-pentanol, 1-hexanol, 1-heptanol, and 1-octanol. The CAE plot is markedly linear, allowing activation energies to be calculated using eq 2. The activation energy from the slope is 25.4 ± 0.7 kJ/mol, while that obtained from the intercept is 25.5 ± 0.8 kJ/mol. The average activation energy calculated for these LiTf solutions is 25.8 ± 0.9 kJ/mol. The application of the CAF to temperature-dependent conductivity data of 0.30 *m* TbaTf-1-alcohol solutions (butanol, pentanol, hexanol, heptanol, and octanol) results in an average activation energy of 43.3 ± 0.8 kJ/mol. A higher E_a value for TbaTf solutions compared to that for LiTf solutions has also been observed for dilute alcohol electrolytes.³ For example, in 0.0055 M 1-alcohol electrolytes, the activation energy for LiTf is 34.9 ± 0.2 kJ mol⁻¹, while that for TbaTf is 39.3 ± 0.4 kJ mol⁻¹. The difference in the E_a value between the two salts may be due to the size and charge density of the cation. We have previously described a transport model based on transition-state theory to address the question, what is thermally activated with activation energy E_a ? For dilute to moderate salt concentrations, an ion is presumed to be surrounded by a group of polar solvent molecules in a liquid electrolyte. This collection of particles is considered to be in a transient, locally stable configuration. The dynamics of the particles are coupled through ion–solvent and solvent–solvent intermolecular interactions. Thermal fluctuations lead to a transient, more open configuration in the vicinity of an ion that facilitates movement of the ion. The higher energy necessary to achieve this fleeting open configuration is the activation energy E_a calculated in the CAF. The system then locally relaxes into a stable configuration. It seems plausible that fewer intermolecular interactions would need to be disrupted for a small particle such as the lithium ion to reach the transition state compared to a much larger ion such as the Tba cation.

The conductivity data of Figure 3 can be explained from the CAF analysis. According to eq 1, the temperature-dependent ionic conductivity has contributions from both the exponential prefactor σ_0 and the Boltzmann factor $\exp(-E_a/RT)$. The Boltzmann factor increases with temperature, but the extent to which this occurs depends on the E_a value. The data show that the exponential prefactor decreases with temperature for both LiTf and TbaTf alcohol electrolytes, as illustrated in Figure 5. The top half of Figure 6 gives the percent increase in the Boltzmann factor for 10 °C temperature increments using activation energy values for both LiTf and TbaTf solutions. A 10 °C increase in temperature from 5 to 15 °C produces a

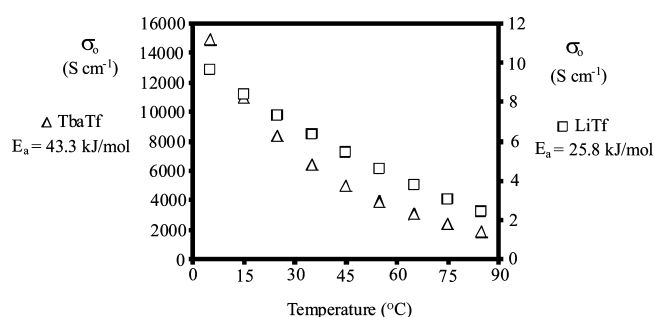


Figure 5. Exponential prefactor versus temperature for 0.30 *m* MX-1-hexanol (MX = TbaTf or LiTf).

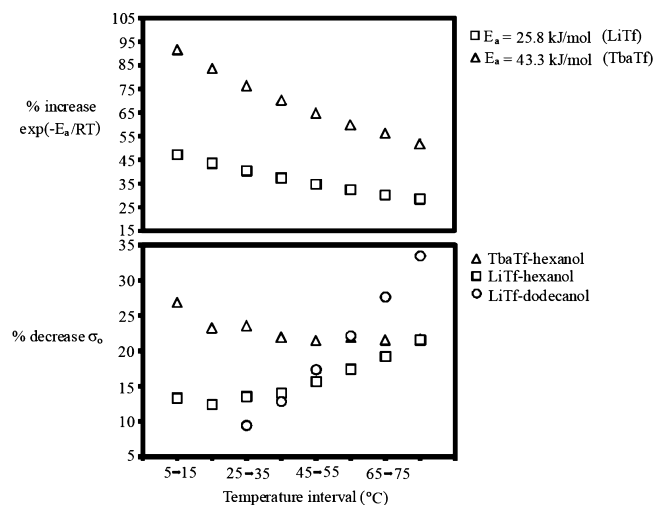


Figure 6. (Top half) Percent increase in $\exp(-E_a/RT)$ for a given 10 °C increase in temperature using the E_a values for both LiTf and TbaTf. (Bottom half) Percent decrease in σ_0 for a given 10 °C increase in temperature for 0.30 *m* solutions of TbaTf-1-hexanol, LiTf-1-hexanol, and LiTf-1-dodecanol.

greater increase in the Boltzmann factor than that for the interval from 75 to 85 °C, regardless of the E_a value. Furthermore, a larger activation energy results in a greater increase in the Boltzmann factor for a given temperature increase. A system with a relatively small energy barrier has a substantial fraction of its particles able to reach a transition state even at low temperature; therefore, increasing the temperature does not shift the distribution of activated species nearly as much as that for a high E_a system where many more particles are confined to the initial state at low temperature.

The bottom half of Figure 6 shows the percent decrease in the exponential prefactor for 10 °C temperature increments for 0.30 *m* solutions of TbaTf-1-hexanol, LiTf-1-hexanol, and LiTf-1-dodecanol. The percent decrease in the prefactor becomes slightly smaller over the temperature range for the TbaTf electrolyte. However, the prefactor decreases to a greater extent at higher temperatures in these LiTf solutions. Consequently, the conductivity of TbaTf in Figure 3 continues to increase even at high temperatures because the increase in the Boltzmann factor far outweighs the decrease in the exponential prefactor. In contrast, the conductivity data of LiTf in Figure 3 levels off at higher temperatures where the increase in the Boltzmann factor is comparable to the decrease in the prefactor. The data in Figure 6 also explain the interesting temperature-dependent conductivity behavior for LiTf-1-dodecanol. The top half of Figure 7 shows that the conductivity for 0.30 *m* LiTf-1-

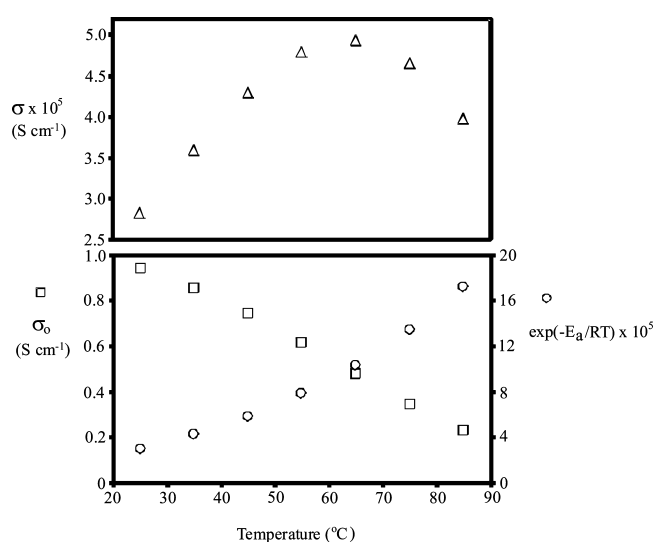


Figure 7. (Top half) Conductivity versus temperature for 0.30 *m* LiTf-1-dodecanol. (Bottom half) Temperature-dependent exponential prefactor σ_0 and Boltzmann factor ($E_a = 25.8$ kJ/mol) for 0.30 *m* LiTf-1-dodecanol.

dodecanol increases with temperature until around 65 °C, but above this temperature, the conductivity decreases with increasing temperature. The decrease in conductivity at higher temperatures can be understood from the bottom half of Figure 7 and the LiTf-1-dodecanol data in Figure 6. At elevated temperatures, the decrease in the exponential prefactor is greater than the increase in the Boltzmann factor; consequently, the conductivity decreases.

4. Ionic Association in LiTf-Dodecanol. Because LiTf is well-known to form ion pairs and aggregates in solution,^{6,7,10} ionic association for the LiTf-dodecanol solution must be examined in order to conclude whether temperature-dependent changes in the number and/or types of species in solution play a significant role in the conductivity behavior observed in Figure 7. Figure 8 shows room-temperature IR spectra in the

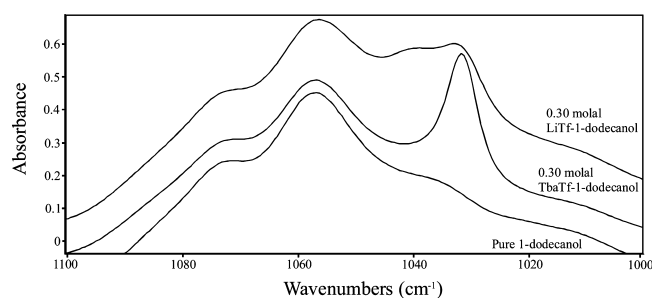


Figure 8. Room-temperature IR spectra in the 1000–1100 cm^{-1} region for pure 1-dodecanol as well as for 0.30 *m* MX-1-dodecanol solutions (MX = LiTf or TbaTf).

1000–1100 cm^{-1} region for pure 1-dodecanol as well as for 0.30 *m* salt-1-dodecanol solutions, where the salt is either LiTf or TbaTf. The frequency of the $\nu_s(\text{SO}_3^-)$ mode of the triflate ion is very sensitive to ionic association.¹⁹ The peak at 1032–1033 cm^{-1} is assigned to the “free” triflate ion.⁷ As noted earlier, the triflate ion is considered free if its interaction with the cation is too weak to alter the electronic distribution within the anion on the time scale of vibrational spectroscopy. The peak at 1040 cm^{-1} is assigned to a contact ion pair.¹⁹ In a contact ion pair,

the cation is directly coordinated to a triflate oxygen atom, which results in a redistribution of charge within the anion that shifts the $\nu_s(\text{SO}_3)$ mode to higher frequencies. Figure 8 shows that a TbaTf-dodecanol solution consists only of free ions because there is only a single triflate ion band at 1032 cm^{-1} . However, the LiTf-dodecanol electrolyte contains both free ions and contact ion pairs because bands are observed at both 1033 and 1040 cm^{-1} , respectively. These spectroscopic data reinforce the distinction between charge-protected and non-charge-protected salts.

It is well-known that the degree of ionic association usually increases as the solution static dielectric constant decreases.²⁰ Because the dielectric constant decreases with increasing temperature for most liquids, it is expected that free ions will be converted into ion pairs and aggregates as the temperature is raised. A curve fitting procedure was used on the $\nu_s(\text{SO}_3)$ mode of the LiTf-dodecanol IR data in order to estimate the fraction of free triflate ions. Table 1 shows the expected trend of

Table 1. Percentage of Triflate Ions That Exist As Free Ions and Contact Ion Pairs at Three Different Temperatures for 0.30 *m* LiTf-1-Dodecanol

temperature (°C)	% free	% contact ion pair
35	60	40
55	57	43
70	54	46

decreasing free ion with increasing temperature. However, the reduction in the free ion is slight and cannot possibly control the conductivity behavior observed in Figure 7. The majority of triflate ions are free in moderately concentrated LiTf-dodecanol solutions, and the fraction of free ion is only expected to increase for the shorter-chain alcohols that have higher dielectric constants.

5. Dependence of σ_0 on ϵ_s for LiTf-Alcohol Solutions.

Previous work has shown that a master curve is formed when the conductivity exponential prefactors are plotted against the dielectric constant for a series of moderately concentrated TbaTf-1-alcohol solutions.⁵ Here, this phenomenon is tested for moderately concentrated LiTf-1-alcohol solutions, which have much stronger ion–ion and ion–solvent interactions compared to TbaTf electrolytes.

Figure 9 plots the temperature-dependent conductivity versus the dielectric constant over the range of 5–85 °C for 0.30 *m* LiTf-1-alcohol solutions. The data are grouped into five distinct curves with each curve consisting of the temperature-dependent data for a given alcohol member. These data are

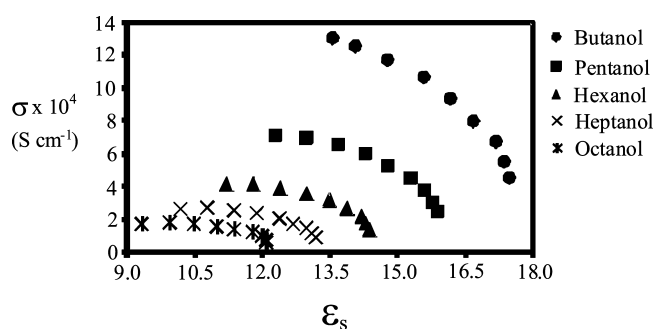


Figure 9. Conductivity versus dielectric constant for 0.30 *m* LiTf-1-alcohol (alcohol = butanol, pentanol, hexanol, heptanol, or octanol).

qualitatively different compared to the corresponding data for moderately concentrated TbaTf-1-alcohol solutions,⁵ which is not surprising considering the different temperature-dependent behavior observed for both the conductivity and dielectric constant between TbaTf and LiTf alcohol electrolytes (Figures 2 and 3). In TbaTf electrolytes, the conductivity increases more gradually with decreasing dielectric constant (increasing temperature) in the high dielectric constant (low temperature) range. In the low dielectric constant (high temperature) range, the conductivity continues to increase with decreasing dielectric constant for TbaTf electrolytes as opposed to the plateau that is observed in Figure 9 for LiTf electrolytes. Dividing the conductivity by the Boltzmann factor $\exp(-E_a/RT)$ gives the exponential prefactor σ_0 . Figure 10 shows that when the

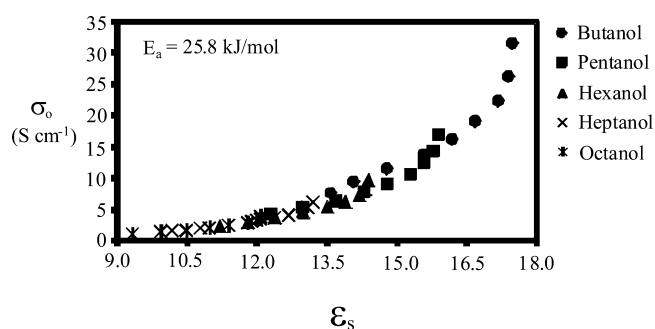


Figure 10. Exponential prefactor σ_0 versus dielectric constant for 0.30 *m* LiTf-1-alcohol (alcohol = butanol, pentanol, hexanol, heptanol, or octanol).

exponential prefactors are plotted against the dielectric constant, a master curve results that is similar in shape to the one observed for TbaTf-1-alcohol electrolytes.⁵ Even though striking differences in the qualitative behavior are observed in both the temperature-dependent conductivity and dielectric constant between TbaTf and LiTf-1-alcohol electrolytes, the qualitative shape of the master curve is very similar for both salt solutions.

SUMMARY AND CONCLUSIONS

Discussion of the data presented in this paper is facilitated by the concept of charge-protected salts and non-charge-protected salts; the distinction between these two cases is described in the text. The two salt systems primarily utilized in this research represent two extreme cases. TbaTf is charge-protected because the charged nitrogen atom is surrounded by four bulky butyl groups, while LiTf undergoes extensive cation–anion and cation–solvent interactions because of the very high, unscreened charge density of the cation. The difference in these two electrolytes is reflected in the contrasting behavior of the static dielectric constant at lower temperatures. The dielectric constants of the LiTf solution and the non-charge-protected NaI solution (Figure 2) increase with roughly the same slope as the temperature is lowered until about 45–50 °C. Then, the rate of increase starts to decrease dramatically with further cooling, and the two curves appear to almost “level off”. Contrasting behavior between TbaTf and LiTf alcohol electrolytes is also observed in the ionic conductivities (Figure 3). The conductivities of both LiTf and TbaTf alcohol solutions increase in a similar fashion from 5 to roughly 35 °C. However, the slope of the conductivity curve of the LiTf solution begins to significantly decrease at about 45 °C, while the

corresponding slope of the TbaTf curve continues to increase with increasing temperature. A similar pattern of behavior is noted in the comparison of the NaI and TbpBF₄ curves (lower portion of Figure 3). A more comprehensive study would be needed to establish that this behavior can be generalized to a wide number of electrolyte systems.

The ionic association that occurs in non-charge-protected electrolytes has been studied by many workers. The degree of ionic association can be extensive, particularly in LiTf-containing electrolytes where ion pairs and more highly associated charged aggregates such as {Li₂Tf}⁺ and {Li₃Tf}²⁺ have been observed.^{7,21} However, the very striking conductivity changes observed in the 0.30 *m* LiTf-dodecanol solution (Figure 7) cannot be interpreted in terms of changes in the nature of the ionic species present over the temperature range of the conductivity data (Table 1). The changes are relatively small and would predict a slight decrease in conductivity over the entire temperature range as the percentage of free ions shows a small decrease. These data suggest that a more important consideration is the strong interaction of a cation with the heteroatoms of the solvent molecules in the LiTf solutions. This interaction is greatly attenuated in the charge-protected TbaTf solutions. Indeed, the importance of cation–solvent interactions has been extensively studied in a wide variety of liquid electrolytes.^{8,9,22–26}

A CAF analysis satisfactorily describes the temperature-dependent conductivity in 1-alcohol electrolytes containing either charge-protected or non-charge-protected salts in terms of the temperature dependence of both the Boltzmann factor and the exponential prefactor. The success of the CAF analysis is most dramatic in the case of LiTf dissolved in long-chain alcohols such as dodecanol, where the conductivity first increases with temperature as expected but then reaches a maximum and then decreases. The relatively large decrease in the exponential prefactor at higher temperatures dominates the increase in the Boltzmann factor, resulting in a conductivity that eventually decreases with increasing temperatures.

AUTHOR INFORMATION

Notes

The authors declare no competing financial interest.

ACKNOWLEDGMENTS

We wish to thank the Army Research Office for support of this work through Grant No. W911NF-10-1-0437. We acknowledge the Johnson research group in the OU physics department, and especially Jeremy Jernigen, for their help with glovebox modifications. We thank Dr. John Furneaux in the OU physics department for designing and implementing the cooling apparatus for the IR measurements. Finally, we acknowledge Chris Crowe for his expertise in software development for the HP 4192A.

REFERENCES

- (1) Petrowsky, M.; Frech, R. *J. Phys. Chem. B* **2009**, *113*, 5996–6000.
- (2) Petrowsky, M.; Frech, R. *J. Phys. Chem. B* **2009**, *113*, 16118–16123.
- (3) Petrowsky, M.; Frech, R. *Electrochim. Acta* **2010**, *55*, 1285–1288.
- (4) Petrowsky, M.; Frech, R. *J. Phys. Chem. B* **2010**, *114*, 8600–8605.
- (5) Fleshman, A.; Petrowsky, M.; Jernigen, J.; Bokalawela, R. S. P.; Johnson, M.; Frech, R. *Electrochim. Acta* **2011**, *57*, 147–152.
- (6) Frech, R.; Huang, W. *J. Solution Chem.* **1994**, *23*, 469–481.
- (7) Frech, R.; Huang, W.; Dissanayake, M. *Mater. Res. Soc. Symp. Proc.* **1995**, *369*, 523–534.
- (8) Bacelon, P.; Corset, J.; Loze, C. *J. Solution Chem.* **1983**, *12*, 13–22.
- (9) Bacelon, P.; Corset, J.; Loze, C. *J. Solution Chem.* **1983**, *12*, 23–31.
- (10) Petrowsky, M.; Frech, R.; Suarez, S.; Jayakody, J.; Greenbaum, S. *J. Phys. Chem. B* **2006**, *110*, 23012–23021.
- (11) Ferry, A.; Jacobsson, P.; Torell, L. *Electrochim. Acta* **1995**, *40*, 2369–2373.
- (12) Stevens, J.; Jacobsson, P. *Can. J. Chem.* **1991**, *69*, 1980–1984.
- (13) Agilent 16452A Liquid Test Fixture Operation and Service Manual; Agilent Technologies: Santa Clara, CA, 2000.
- (14) Cachet, H.; Cyrot, A.; Fekir, M.; Lestrade, J. *J. Phys. Chem.* **1979**, *83*, 2419–2429.
- (15) Gestblom, B.; Svorstol, I.; Songstad, J. *J. Phys. Chem.* **1986**, *90*, 4684–4686.
- (16) Sigvartsen, T.; Gestblom, B.; Noreland, E.; Songstad, J. *Acta Chem. Scand.* **1989**, *43*, 103–115.
- (17) Paolantoni, M.; Sassi, P.; Morresi, A.; Cataliotti, R. *Chem. Phys.* **2005**, *310*, 169–178.
- (18) Palombo, F.; Tassaing, T.; Danten, Y.; Besnard, M. *J. Chem. Phys.* **2006**, *125*, 094503–1–094503–8.
- (19) Schantz, S.; Sandahl, J.; Borjesson, L.; Torell, L.; Stevens, J. *Solid State Ionics* **1988**, *28–30*, 1047–1053.
- (20) Bockris, J.; Reddy, A. *Modern Electrochemistry*, 2nd ed.; Plenum Press: New York, 1998; Vol. 1, sections 3.8.1–3.8.5.
- (21) Huang, W.; Frech, R.; Wheeler, R. A. *J. Phys. Chem.* **1994**, *98*, 100–110.
- (22) Bockris, J.; Reddy, A. *Modern Electrochemistry*, 2nd ed.; Plenum Press: New York, 1998; Vol. 1, Chapter 2.
- (23) James, D. *Prog. Inorg. Chem.* **1985**, *33*, 353–391.
- (24) Wang, Z.; Huang, B.; Xue, R.; Chen, L.; Huang, X. *J. Electrochem. Soc.* **1998**, *145*, 3346–3350.
- (25) Chang, T.; Irish, D. *J. Solution Chem.* **1974**, *3*, 161–174.
- (26) Mollner, A.; Brooksby, P.; Loring, J.; Bako, I.; Palinkas, G.; Fawcett, W. *J. Phys. Chem. A* **2004**, *108*, 3344–3349.